Bridge on a chip: realization of a Kelvin bridge based on quantum Hall elements for resistance calibration

(Article begins on next page)

18 December 2025

Bridge on a chip: realization of a Kelvin Bridge based on quantum Hall elements for resistance calibration

M. Marzano, M. Kruskopf and A. R. Panna

M. Marzano

Politecnico di Torino, Dipartimento di Elettronica e Telecomunicazioni
Torino, Italy
Istituto Nazionale di Ricerca Metrologica (INRIM), Division of Quantum Metrology and Nanotechnologies,
Torino, Italy

M. Kruskopf

University of Maryland, Joint Quantum Institute,
College Park, MD, US

A. R. Panna

National Institute of Standards and Technology,
Gaithersburg, MD, US

Summary. — We report an implementation of a Kelvin bridge incorporating three SiC/EG quantized Hall resistance standards in an on-chip triple series connection. The bridge is functionalized at the $i = 2$ plateau index of the von Klitzing constant, $R_{\mathrm{K}} = h/e^2$, and is used to calibrate a four-terminal resistance standard with a nominal value close to $R_{\mathrm{K}}/2$. This work demonstrates that a quantum Hall Kelvin bridge can reach a calibration standard uncertainty better than 10^{-8} using a commercial off-the-shelf voltmeter and current source and that its performance rivals present-day direct and cryogenic current comparators.

1. – Introduction

National Metrology Institutes (NMIs) exploit the quantum Hall effect (QHE) to realize the unit of resistance [1]. Common traceability chains start with the calibration of an artefact resistance standard from the quantized Hall resistance $R_{\mathrm{H}} = h/(2e^2) \approx 12\,906.4037\,\Omega$ produced by a single QHE element. The calibration is performed by means of a resistance bridge, and the artefact resistance standards of interest have nominal values in decadal sequence $(100\,\Omega,\ 1\,\mathrm{k}\Omega,\ \dots)$ or equal to R_{H} [2].

The highest accuracy, around 10^{-9}, is achieved with resistance bridges based on the cryogenic current comparator (CCC) [3]. The CCC operates in a low-noise, low-magnetic field liquid helium cryogenic environment, necessarily independent of the one where the QHE is realized. A dedicated room-temperature direct current comparator (DCC) bridge can be also employed to perform the calibration, though this is limited by the low current in the QHE device and the measurement accuracy, at the 10^{-8} level [4]. Both CCC and DCC bridges are expensive instruments.

This work presents the design of a DC quantum Hall Kelvin bridge for the direct calibration of standard resistors against a quantum Hall resistance standard [5] and its first implementation at the National Institute of Standards and Technology (NIST), Gaithersburg, MD, US [6].

The bridge design is simple and involves a minimal number of instruments. The bridge reading is the deviation from equilibrium. The bridge implementation is based on a quantum Hall array resistance standard (QHARS) composed of three graphene QHE elements and superconducting wiring. The bridge calibrates a $12\,906\,\Omega$ standard resistor with a standard uncertainty of a few parts in 10^9, comparable with that of the bridges traditionally employed in such calibrations.

2. – Traditional Kelvin bridge

Two four-terminal low resistances R_1 and R_x can be compared with a Kelvin bridge [7], schematically shown in fig. 1. This bridge can be reduced to a conventional Wheatstone
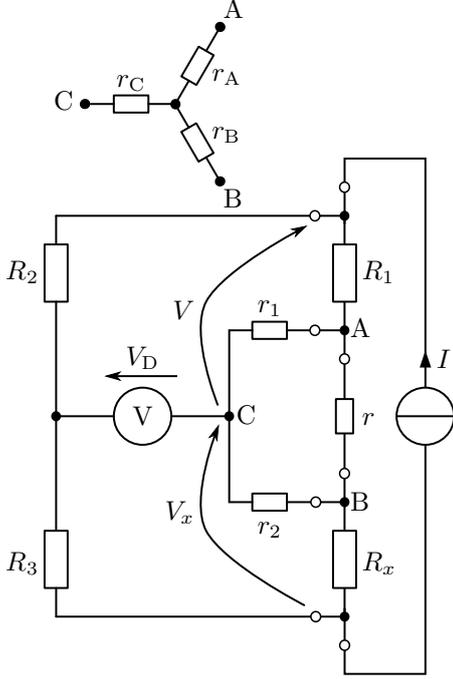
Fig. 1. – Schematic of a traditional Kelvin bridge. The resistances r_1 and r_2 compose the *Kelvin arm*, and r represents the stray resistance between the nodes A and B. The top inset represents the resistances r_A, r_B and r_C resulting from a Δ-Y transformation of r_1, r_2 and r.
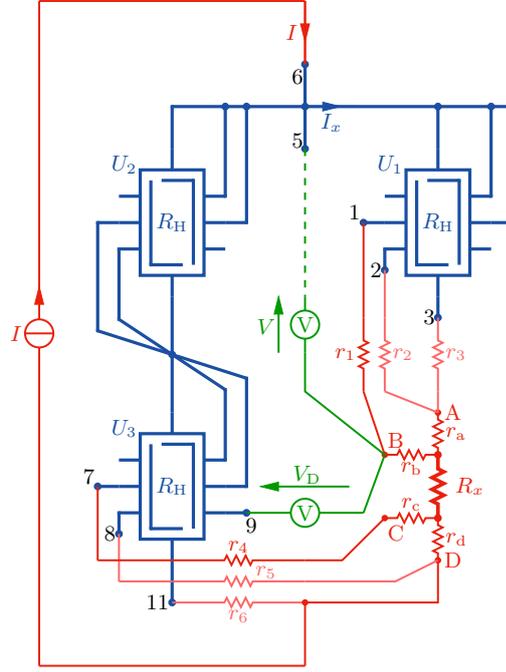
Fig. 2. – Schematic of the quantum Hall Kelvin bridge with the major stray resistances. The bridge is composed of three triple-series and -parallel interconnected QHE elements U_1, U_2 and U_3, and of the four-terminal resistor under calibration R_x. I is the bridge excitation current, V is the voltage drop across U_1 and V_D is the unbalance voltage. Blue elements represent the device; red elements are external to the device. From [6] ©*BIPM & IOP Publishing Ltd. Reproduced by permission of IOP Publishing. All rights reserved.*

bridge with a Δ-Y transformation of r_1, r_2 and r into $r_A = rr_1/(r + r_1 + r_2)$, $r_B = rr_2/(r + r_1 + r_2)$ and $r_C = r_1r_2/(r + r_1 + r_2)$, as shown in the top inset of fig. 1. The bridge balance equation becomes

$$(1) \qquad \frac{R_1 + r_A}{R_x + r_B} = \frac{R_1(r + r_1 + r_2) + rr_1}{R_x(r + r_1 + r_2) + rr_2} = \frac{R_2}{R_3}.$$

This equation is independent of r when the *Kelvin condition* $r_1/r_2 = R_1/R_x = R_2/R_3$ holds. When this condition is not fulfilled, there is an error that depends at first order on the stray resistances.
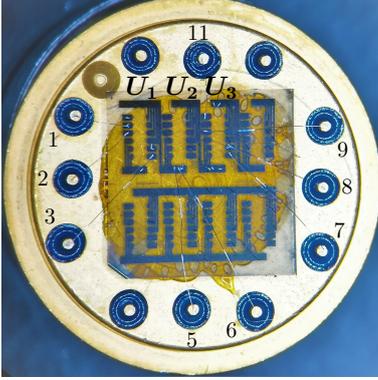
Fig. 3. – The sample is composed of multiple-series and -parallel interconnected graphene Hall bars and is mounted on a TO-8 header. Only U_1, U_2 and U_3 are employed in the present implementation.
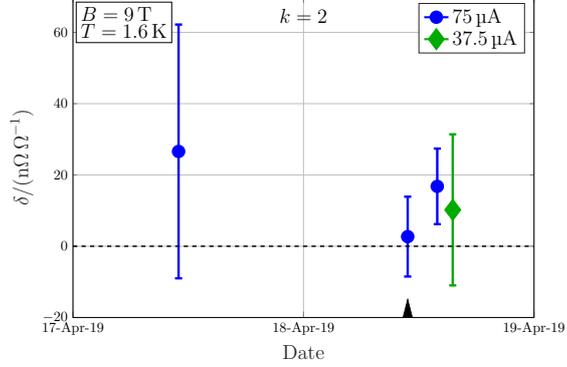

Fig. 4. – Summary plot of the final results of four comparisons. δ represents the difference between the calibration performed with the quantum Hall Kelvin bridge and that with the CCC. The uncertainty bars represent the expanded uncertainties with coverage factor $k = 2$. From [6] ©*BIPM & IOP Publishing Ltd. Reproduced by permission of IOP Publishing. All rights reserved.*

The Kelvin bridge can also be operated in the *deflection mode*, where a resistance ratio is related to the unbalance voltage V_D. In the special case of equal arms, $R_1 = R_2 = R_3 = R_\mathrm{H}$, and $R_x = R_\mathrm{H}(1 + x)$, where x is the relative deviation of R_x from R_H, the relationship between x and V_D can be written as

$$(2) \qquad x = -2\frac{V_\mathrm{D}}{V} - \frac{1}{R_\mathrm{H}}(r_\mathrm{B} - r_\mathrm{A}).$$

3. – Theory of operation

Figure 2 represents the schematic of the quantum Hall Kelvin bridge with the major stray resistances. The bridge is composed of three QHE elements U_1, U_2 and U_3, joined by multiple connections [8], and of the four-terminal resistor under calibration $R_x = R_\mathrm{H}(1 + x)$. The lead resistances from the QHE elements to the junction terminals A, B, C and D are labelled from r_1 to r_6; the lead resistances from the junction terminals to R_x are labelled from r_a to r_d.

The bridge is driven by the current I, which splits between the two bridge arms. The current I_x is that crossing U_1 and R_x, and $V = R_\mathrm{H}I_x$ is the Hall voltage measured across U_1. The bridge operates in the deflection mode and V_D is the bridge unbalance voltage.

The measurement model can be obtained with the methods developed in [5, 9, 10],

$$(3a) \qquad\qquad x = -2\frac{V_{\mathrm{D}}}{V} - \Delta x^{\mathrm{leads}},$$

$$(3b) \qquad \text{with} \qquad \Delta x^{\mathrm{leads}} = \frac{1}{R_{\mathrm{H}}^2}\left[r_{\mathrm{a}}(r_{\mathrm{b}} - r_1) + (r_{\mathrm{c}} + r_4)r_{\mathrm{d}}\right] + O\left(\frac{r_{\mathrm{max}}}{R_{\mathrm{H}}}\right)^3.$$

The error term $\Delta x^{\mathrm{leads}}$ depends at second order on the lead resistances r_1, r_{a}, r_{b}, $r_{\mathrm{c}} + r_4$, and r_{d}. Instead, the resistances r_2, r_3, r_5 and r_6 contribute only at third order, as expected from a triple-series connection. r_{max} is the maximum lead resistance of a connection and the *big O notation* specifies the limit on the growth rate of the higher-order terms. This contrasts favourably with the result of the traditional Kelvin bridge, eq. (2), where the error is at first order in the stray resistances.

4. – Implementation and results

The quantum Hall Kelvin bridge is implemented with the QHARS shown in fig. 3, composed of three multiple-series and -parallel interconnected graphene Hall bars. To reduce the effect of contact and lead resistances, split contacts [11] and superconducting interconnections are employed [12]. The device thus differs from a conventional one for being crossover free.

The bridge operates in a cryogenic system at about 1.5 K and at a magnetic flux density of 9 T. The four-terminal resistor under calibration R_x is a 12.906 kΩ resistance standard kept in a temperature-controlled oil bath at 25 °C.

A direct current standard generates the bridge excitation current I and a nanovoltmeter alternatively measures the voltages V and V_{D}. The measured data are acquired with a purpose-coded application.

Figure 4 reports the results of a comparison between a calibration of R_x with the quantum Hall Kelvin bridge and one with a CCC bridge. These results show that the bridge can calibrate a resistor having nominal value R_{H} with a relative uncertainty of a few parts in 10^9, thus comparable with that of the CCC bridge [4] employed during the validation measurements.

5. – Conclusions

We presented here an alternative method to calibrate a 12.906 kΩ resistance standard directly against the quantized Hall resistance. This method is competitive with state-of-the-art resistance bridges and it can be further extended to include QHARSs [13, 14] in place of the individual elements, thus allowing the calibration of resistance standards having nominal values different from R_{H}, like decadal ones.

<p align="center">* * *</p>

Maryland, College Park, MD, US), L. Callegaro (INRIM, Turin, Italy) and M. Ortolano (Politecnico di Torino, Turin, Italy). Martina Marzano thanks R. E. Elmquist and the Fundamental Electrical Measurements Group for supporting her stay at NIST, Gaithersburg, MD, US, and this work.

REFERENCES

[1] Bureau International des Poids et Mesures, 9th SI brochure (2019).
[2] Chua S. W., Kibble B. P. and Hartland A., *IEEE Trans. Instrum. Meas.*, **48** (1999) 342.
[3] Williams J., *IET Science, Measurement & Technology*, **5** (2011) 211.
[4] Panna A. R., Kraft M. E., Rigosi A. F., Jones G. R., Payagala S. U., Kruskopf M., Jarrett D. G. and Elmquist R. E., *Uncertainty of the ohm using cryogenic and non-cryogenic bridges*, in proc. of *2018 Conference on Precision Electromagnetic Measurements (CPEM 2018)* (Paris, France) 2018, pp. 1–2.
[5] Marzano M., Callegaro L. and Ortolano M., *A quantum Hall effect Kelvin bridge for resistance calibration*, in proc. of *2018 Conference on Precision Electromagnetic Measurements (CPEM 2018)* (Paris, France) 2018, pp. 1–2.
[6] Marzano M., Kruskopf M., Panna A. R., Rigosi A., Patel D. K., Jin H., Cular S., Callegaro L., Elmquist R. E. and Ortolano M., *Metrologia*, (2019) , in press.
[7] Callegaro L., *Electrical impedance: principles, measurement, and applications*, in Sensors (CRC press: Taylor & Francis, Boca Raton, FL, USA) 2013, iSBN: 978-1-43-984910-1.
[8] Delahaye F., *J. Appl. Phys.*, **73** (1993) 7914.
[9] Ortolano M. and Callegaro L., *Metrologia*, **49** (2012) 1.
[10] Marzano M., Oe T., Ortolano M., Callegaro L. and Kaneko N. H., *Metrologia*, **55** (2018) 167.
[11] Kruskopf M., Rigosi A. F., Panna A. R., Patel D. K., Jin H., Marzano M., Berilla M., Newell D. B. and Elmquist R. E., *IEEE Trans. Electron Devices*, **66** (2019) 3973.
[12] Kruskopf M., Rigosi A. F., Panna A. R., Marzano M., Patel D., Jin H., Newell D. B. and Elmquist R. E., *Metrologia*, **56** (2019) 065002, accepted.
[13] Piquemal F. P. M., Blanchet J., Gèneves G. and André J.-P., *IEEE Trans. Instr. Meas.*, **48** (1999) 296.
[14] Ortolano M., Abrate M. and Callegaro L., *Metrologia*, **52** (2015) 31.